

**Optical systems for point-of-care diagnostic instrumentation: analysis of imaging performance and cost**

Mark C. Pierce<sup>a</sup>, Shannon E. Weigum<sup>b</sup>, Jacob M. Jaslove<sup>a</sup>, Rebecca Richards-Kortum<sup>b,c</sup>, Tomasz S. Tkaczyk<sup>b,d\*</sup>

- a) Department of Biomedical Engineering, Rutgers, The State University of New Jersey, 599 Taylor Road, Piscataway, NJ 08854
- b) Department of Bioengineering, Rice University, 6100 Main Street, Houston, TX 77005
- c) Rice 360° - Institute for Global Health Technologies, Rice University, 6500 Main Street, Houston, TX 77030
- d) Department of Electrical and Computer Engineering, Rice University, 6100 Main Street, Houston, TX 77005

\* Corresponding author: Tomasz S. Tkaczyk, Department of Bioengineering, Rice University, 6100 Main St, Houston, TX, 77005, email: [ttkaczyk@rice.edu](mailto:ttkaczyk@rice.edu), phone: 1-713-348-4362, fax: 1-713-348-5877

**Abstract and key terms:**

One of the key elements in point-of-care (POC) diagnostic test instrumentation is the optical system required for signal detection and / or imaging. Many tests which use fluorescence, absorbance, or colorimetric optical signals are under development for management of infectious diseases in resource limited settings, where the overall size and cost of the device is of critical importance. At present, high-performance lenses are expensive to fabricate and difficult to obtain commercially, presenting barriers for developers of *in vitro* POC tests or microscopic image-based diagnostics. We recently described a compact “hybrid” objective lens incorporating both glass and plastic optical elements, with a numerical aperture of 1.0 and field-of-view of 250  $\mu\text{m}$ . This design concept may potentially enable mass-production of high-performance, low-cost optical systems which can be easily incorporated in the readout path of existing and emerging POC diagnostic assays.

In this paper, we evaluate the biological imaging performance of these lens systems in three broad POC diagnostic application areas; (1) bright field microscopy of histopathology slides, (2) cytologic examination of blood smears, and (3) immunofluorescence imaging. We also break down the fabrication costs and draw comparisons with other miniature optical systems. The hybrid lenses provided images with quality comparable to conventional microscopy, enabling examination of neoplastic pathology and infectious parasites including malaria and cryptosporidium. We describe how these components can be produced at below \$10 per unit in full-scale production quantities, making these systems well suited for use within POC diagnostic instrumentation.

Key terms: POC optics, Miniature optics, Cost assessment, Diagnostic imaging performance

**Introduction:**

Optical detection and imaging strategies based upon techniques including absorbance<sup>30</sup>, fluorescence<sup>27,28,32</sup>, chemiluminescence<sup>36</sup>, interferometry<sup>37</sup>, and surface plasmon resonance<sup>11</sup> have been employed in point-of-care (POC) diagnostic test development. Optical techniques are often preferred over electrochemical detection due to their high sensitivity, capacity for quantitative output, compatibility with bench-top assays, and potential for multiplexed detection of several targets in a single sample<sup>26</sup>. At present, many POC test developers have limited access to small, high-quality, portable optical detection devices for use in the field, and therefore, rely on traditional microscopes or bulky optical readers<sup>21,35</sup>. While these systems can be used to generate high quality, quantitative data, they are often expensive and must be used with large format cameras and detectors that require access to stable electrical power, neither of which may be available in remote settings.

An alternative approach has been to develop highly specialized microfluidic chips with integrated optical readout systems. The advantage of this method is that the complete assay can be contained on the chip, which can then be disposed of after a single use<sup>7,26</sup>. However, such solutions are highly customized and require complete redesign and manufacturing process development for each new application. This significantly lowers potential production quantities and it can be prohibitively expensive to fabricate small quantities of devices for field evaluation of a prototype design.

A third approach which can be applied to conventional pathology and cytology-based diagnostics involves the design of classical microscope platforms which provide high-resolution images, but do so in a ruggedized form and at greatly reduced cost<sup>24,25</sup>. However, the resulting microscope platform can still be bulky, and often requires a trained microscopist to acquire and

interpret the images. Such an approach may be appropriate for central referral facilities which have access to trained personnel, but distributed microscopy is much more difficult to implement at the point-of-care.

A recently emerging class of optical read out for POC instruments takes advantage of widespread diffusion of consumer electronics, often in the form of portable cell phones<sup>38</sup>. One approach involves using a cell phone camera to directly image samples by placing additional lenses in front of the built-in camera lens to increase magnification. Cell phone microscopy is simple and also allows for on-phone image processing or rapid transmission of images to a central facility for analysis. While some groups have built cell phone attachments which use conventional microscope objective lenses<sup>5</sup>, others have adopted the simple approach of placing a single lens element between the phone camera and the sample<sup>31,39</sup>. The additional lens or lens system can be connected directly to the phone, or alternatively placed directly on top of the sample<sup>1</sup>, allowing the device to interface with any phone camera without being specifically designed to fit the phone body.

A related but distinct approach is lens-free holography in which specimens are placed directly in front of a CMOS image sensor. The sample is placed either directly on top of or within a few millimeters of the sensor and images are reconstructed based on the shadows and diffraction patterns projected onto the sensor<sup>13,20</sup>. Spatial resolution of 225 nm has been achieved using this technique by combining data from multiple images with different illumination patterns to overcome the limits imposed by the sensor pixel size<sup>14,23</sup>. Color images can also be obtained using lensless holography with the addition of an extra processing step<sup>15</sup>. Devices based on this principle can be well-suited for POC applications since they are relatively

inexpensive and provide a very large field of view while maintaining a high resolution, which can allow for high-throughput assessment of large numbers of cells in a sample.

Despite these advances in optical detection methods, many potentially promising diagnostic tests are not translated from the lab to resource-poor settings, where high optical performance at minimal cost is essential. In order to overcome this barrier, high-quality, cost-effective optics are needed, both for image-based diagnostics (eg. pathology / cytology) and for radiometry-based tests (eg. ELISA / colorimetric platforms). To encourage widespread uptake and deployment in the field, these components must be affordable, highly scalable in production, and broadly compatible with different assays and detection modalities.

We recently described a novel design for creating miniature objective lens systems which could potentially be very cost-effective<sup>18,19</sup> (Fig. 1a). By combining an off-the-shelf glass lens with injection-molded plastic lenses, we significantly reduced overall component costs while maintaining high-quality imaging performance. Integration of self-centering optomechanical mounting elements simplified the assembly process by eliminating the need for labor-intensive optical alignment, further reducing expenses. The small size, low-cost, and straightforward assembly features potentially make these “hybrid” glass-plastic lens systems ideal building blocks for optical detection and imaging in POC assays. In this paper, we present the first biological demonstrations of these lens systems for use in POC instrumentation. We evaluate the optical image quality for microscopic examination of infectious and non-infectious diseases relevant to POC applications by comparison with a conventional bench-top microscope. We then examine the requirements for mass producing these lenses and develop price estimates for large scale production using various candidate fabrication and assembly methods.

## **Materials and Methods:**

### *Optical systems*

The hybrid objective lens systems were fabricated and assembled as described previously<sup>19</sup>. As a quantitative measure of optical quality, the Strehl ratio was determined by using the slanted edge modulation transfer function technique. All biological specimens were illuminated in the Köhler configuration for transmitted light (bright field) microscopy, or in the epi-configuration for fluorescence microscopy. For image capture, the image of the specimen formed by the hybrid objective lens system (3.3x magnification) was re-imaged onto a CCD camera (Zeiss, MRc5) with an infinity-corrected 10x / 0.45 microscope objective and tube lens, resulting in total magnification (at the camera plane) of 33x. A schematic diagram of this experimental configuration is shown in Fig. 1b. Conventional microscope images were collected using a Zeiss Axiovert 200M inverted microscope with 20x / 0.75 or 40x / 0.95 plan-apochromat objectives and color CCD camera (Zeiss, MRc5). The technical specifications of the hybrid objective lens being studied, and the commercial Zeiss objectives are listed in Table 1.

### *Biological specimens*

Microscopy and imaging remain one of the most widely used and trusted techniques for diagnosing infectious and non-infectious diseases worldwide. Table 2 provides a summary of five commonly encountered infectious diseases which are targets for POC test developers. The table includes the spatial characteristics of the target species and also the currently recommended parameters for microscope-based diagnosis (magnification and number of fields). We examined the diagnostic imaging quality of the hybrid objective lens for three important POC microscopy applications. Human pathology slides from the buccal mucosa were obtained from The University of Texas M. D. Anderson Cancer Center (IRB Protocol #04-0491) and stained using

hematoxylin and eosin (H&E) according to standard histology protocols. Teaching slides containing human blood infected with *Plasmodium falciparum* parasites in a Giemsa-stained thin smear preparation were obtained from McGill University Centre for Tropical Diseases, Montreal, Quebec. *Cryptosporidium parvum* parasites ( $\sim 1 \times 10^6$  oocysts/mL) were provided by A. Clinton White Jr. of The University of Texas Medical Branch, Department of Infectious Disease, Galveston, TX. Fluorescent immunolabeling of these parasites was performed using an anti-Cryptosporidium monoclonal antibody directly conjugated to Alexa Fluor<sup>®</sup>488 (AbD Serotec, #2402-3007A488) according to the manufacturer's flow cytometry protocol. A wet-mount slide of the stained oocysts was prepared for microscopic examination.

## Results:

The incidence of cancer in developing countries has risen sharply over the past few decades and this trend is expected to continue<sup>4</sup>. Nearly two-thirds of the 7.6 million cancer-related deaths worldwide every year now occur in low- and middle-income countries, making early cancer detection a major health priority in these settings<sup>12</sup>. Figure 2 presents bright-field histopathology images of H&E stained specimens from the oral cavity acquired with the hybrid objective (Fig. 2a) and a 40x / 0.95 Zeiss microscope objective (Fig. 2b). The hybrid objective is capable of resolving cellular and subcellular features, such as nuclear size, shape, texture, and tissue architecture, which are important markers for diagnosis of dysplasia and cancer<sup>17</sup>. To quantitatively compare the performance of both systems, the nuclear-to-cytoplasm area ratio (N/C ratio) was calculated as a function of depth beneath the epithelial surface. Identical sample areas were selected for both modalities and the N/C ratio was calculated by automated image analysis for regions of interest vs. depth; results are shown in Fig. 2c. This procedure involved simple intensity thresholding and morphological processing to identify nuclei in each image. Good agreement was observed between data obtained with both the miniature and commercial optical systems, suggesting that the miniature system has sufficient performance to allow accurate assessment of N/C ratio and possibly even provide a degree of automated analysis.

Detection of malaria is one of the most critical POC diagnostic needs in developing countries. We evaluated the hybrid objective for bright-field imaging of blood smears containing the malaria parasite *P. falciparum* against standard microscope imaging (40x / 0.95 objective), as illustrated in Fig. 3. With both systems, the immature trophozoite, or ring stage, of the parasite is visible within infected red blood cells (Fig. 3a,b, arrows). The delicate ring stage is the most



common form of the parasite found in peripheral blood and is particularly important for determination of parasitemia and speciation based upon their distinctive morphology<sup>34</sup>. To quantitatively assess the performance of both systems in malaria diagnostics three malaria samples were evaluated. Two matching fields of 100  $\mu\text{m}$  x 100  $\mu\text{m}$  (for both the hybrid objective and Zeiss microscope) were evaluated in two independent manual counting procedures. Figure 3c summarizes results of this evaluation, comparing malaria counts for both systems across three samples. Again, good qualitative and quantitative agreement between both systems suggest that the hybrid miniature objective may be suitable for use in instruments designed for field diagnosis of malaria in POC settings.

The third POC application evaluated with the hybrid objective was detection of the intestinal protozoa *Cryptosporidium*, using a fluorescence immunoassay. *Cryptosporidium* is a significant cause of chronic diarrhea in developing countries, contributing to malnutrition and high diarrhea-related morbidity and mortality in children and immune deficient adults<sup>29</sup>. Detection is important for treatment selection and control of waterborne outbreaks. Figure 4 presents fluorescence images of stained *C. parvum* oocysts acquired with the miniature objective (Fig. 4a) and the Zeiss 40x / 0.95 microscope objective (Fig. 4b). With both systems, individual or clustered protozoan oocysts can be resolved and exhibit a similar localization pattern expected for an extracellular surface label (i.e. bright edges and dim interior). Figure 4c demonstrates selected image zones with cross-sectional intensity profiles through oocysts. Images obtained with the hybrid objective exhibit lower signal level and higher background, but still demonstrate similar morphology to those acquired with the Zeiss system.

## **Discussion**

We previously reported the design and assembly methods for several miniature objective lenses developed by our group over the past ten years (Fig. 1a), each of which used different materials and fabrication techniques<sup>9,18,19,22</sup>. These lens systems have similar specifications (numerical aperture of 1.0, field-of-view of 250  $\mu\text{m}$ , and outer diameter less than 10 mm), yet they differ significantly in their cost and potential for mass production (Table 1). Objective (I) in Fig. 1a contains eight individual glass lenses, each fabricated using conventional grinding and polishing methods and aligned with high-precision metal opto-mechanics within a 7 mm diameter brass housing<sup>22</sup>. This system demonstrated diffraction-limited imaging, but the final cost of a single objective was \$8,000. Objective (II) was designed with five plastic lenses, each made by injection-molding<sup>9</sup>. This fabrication approach also allowed mounting and alignment features to be molded into the individual components and incorporation of aspheric surfaces, which in turn reduced the total number of individual lenses required for each objective. This all-plastic objective exhibited near diffraction-limited imaging with a fabrication cost estimated at \$250 (in volumes of 10,000). In order to bring the single unit cost to a target of below ten dollars for POC applications<sup>10</sup>, we aimed to reduce both the cost of the individual components and the cost of assembly processes. This approach resulted in the “hybrid” design used here, which combined glass and plastic lenses, mounted in optomechanical components made by X-ray or UV lithography (objective III in Fig. 1a). The self-centering optomechanics inherently provide positional tolerances of better than 10  $\mu\text{m}$ , removing the need for precision alignment equipment and skilled handling for assembly. This third objective contains one glass lens, two plastic lenses, and seven optomechanical elements, all assembled within a 10.4 mm length of hypodermic tubing. As demonstrated by the image data in Fig’s 2-4, and a measured Strehl ratio of 0.75, this objective exhibits excellent optical performance. Next, we analyze the complete

fabrication and assembly costs for this particular hybrid lens system in prototype and production volumes, demonstrating that these systems may be realized at extremely low costs for integration into POC instrumentation. The following cost analysis is based on our direct experience, our internally developed processes, information from vendors, and knowledge acquired while applying these technologies to construct miniature microscopes for medical diagnostics.

The fabrication cost of this objective in volumes of 10,000 is estimated to be around \$102, with the breakdown in Table 3 indicating that the optomechanical components represent the largest contribution to overall cost. This is due to the lithographic fabrication process for these parts requiring an initial investment in a mask costing \$6,000 for a 4" wafer or \$8,000 for a 6" wafer (Center for Advanced Structures and Devices, LA, USA). Once a mask has been acquired, X-ray and UV lithography facilities with the capability of electroplating are available at Honeywell (Kansas City, USA) or the Institut für Mikrotechnik Mainz GmbH (Mainz, Germany). Although a 4" mask is less expensive, it can only generate about 300 optomechanical components in a single production run, while the 6" mask can produce 1,200 components per run, significantly reducing the per part cost. The X-ray exposure and electroplating costs for the 4" mask is \$2,000 and for the 6" mask is \$2,500 for low volume. These figures decrease to \$350 to \$400 per run for production levels yielding in the region of 1-3 million components per year. The fixturing equipment required to remove individual parts from the substrate following lithography costs \$1,000 for both processes. Oxidation to blacken mounting parts to reduce light scattering within the objective adds an additional \$200 per batch (based on processing currently performed in-house). Taking each of these factors in to account, the cost of fabricating the optomechanical components is approximately \$30 / part and \$10 / part when using 4" and 6"

masks, respectively (Table 4). The total cost for the seven optomechanical parts required for each objective is then \$210 or \$70. The X-ray process employed in fabricating the optomechanics for the objective lenses used here is advantageous for prototyping and for low- to mid-volume production, as it allows high yields to be obtained with low risk. For higher volume production, UV lithography with lower per-run costs may replace X-ray processing once the volume justifies the increased process optimization effort. While lower than in previous designs, the assembly cost is still a significant contributor to the total cost. Therefore for large volumes (> 1000), an automated fixturing and batch assembly process is required to maintain assembly costs at approximately \$1-5 per unit (for low volumes, the assembly cost is related to the technician's labor over 15-60 minutes). Single glass lenses from commercial vendors cost approximately \$30-\$40 in small quantities and about 40% less if quantities larger than around 50 are purchased. Unit costs for quantities over 1,000 can be decreased further, especially if acquired directly from glass press-molding facilities. Plastic injection molding lenses can be produced for a few cents each, based on material costs for optical media grade polycarbonate (\$1.92 /lb) or crystal high-impact polystyrene (\$0.95 /lb). The single shot (per lens) cost would be then \$0.06 for polycarbonate and \$0.03 for polystyrene, assuming a shot size of 0.03125 lbs<sup>16</sup>. The typical injection molding facility (for example, based on use of a 17-ton RoboShot machine) would allow for 45 second cycle times, or 79 parts per hour, 632 parts per 8 hr day, and 3,160 parts per 5 day week. At full capacity, 151,680 parts would be made per year (48 weeks operation). Cycle times could be reduced down to 2-5 seconds with a fully automated part ejection system, and in addition, multiple components can be produced during each cycle. The cost of applying anti-reflection or filter coatings to optics is typically related to the number of process runs required and can be very low for these systems, since individual part dimensions are

relatively small. Coating would cost approximately \$500-\$2000 for a single process, increasing to \$1,000-\$5,000 for multi-layer coating processes (these data are based upon past fabrication costs through AccuCoat Inc.). Typical vacuum chamber coating can accommodate over 500 small parts in a single coating run, resulting in overall coating costs below \$1.

Based on these estimations, a cost summary for the hybrid objective lens system used in Fig's 2-4 is shown as a function of manufacturing volume in Fig. 5. Figure 5a presents costs for prototyping or low volume fabrication, while Fig. 5b shows cost per unit in high production volumes using the technologies described above. For prototype quantities (50-200 units), the use of diamond-turned lenses removes the burden of purchasing an expensive mold for injection molding, enabling miniature integrated prototypes to be assembled for \$500-\$725. At higher production quantities, the use of injection molding becomes highly beneficial and is essential if the cost per objective is to be brought below \$100. If the opto-mechanical parts are made with an optimized UV process (approx. 1 million units) and batch assembly techniques, this overall cost per objective can be reduced to the \$5-10 range. Note that as each objective requires between 6 and 10 optomechanical parts, the actual production quantity of complete objective systems only needs to be one order of magnitude smaller to achieve these cost savings. This is significant, considering that off-the-shelf microscope objectives with numerical aperture around 1.0 currently cost in the \$1,000-\$4,000 range. Gradient refractive index (GRIN) lenses also offer the potential for high resolution imaging in a small diameter micro-optic. However, individual GRIN lenses generally have NA values below 0.6 and significant aberrations, limiting the achievable resolution. A hybrid approach to address these issues was described by Baretto *et al.*<sup>2</sup>, who used GRIN lenses and traditional refractive lenses to acquire two-photon images with

low aberrations at NA 0.82. Similar systems are available commercially, costing approximately \$1,000 (if purchased individually), providing diffraction limited imaging over a 50-100  $\mu\text{m}$  field. However, to in order to reach this cost level, the minimum cost of setting up production (assuming an existing facility) is about \$250k-\$500k. For the miniature objectives used here, at higher production quantities, the true benefits of injection molding, UV lithography, and batch assembly can be fully realized, such that the total objective cost is estimated to be slightly above \$10 for  $\geq 100,000$  units, and below the \$9-10 range for  $\geq 1$  million units (Table 3).

We have demonstrated that objective lenses designed using a novel hybrid optics / optomechanics concept can be used to acquire high-quality images in three classes of assay encountered in POC diagnostics. We have also described how the underlying fabrication and assembly processes can be structured to yield individual units at a price point around \$10. As suggested by the data in Fig's 2-4, the performance and price point demonstrated here may be most appropriate in applications which currently employ either conventional or compact microscope systems for image-based diagnostics. Further, the size of these optical systems raises the possibility of designing imagers for pathology and cytology which are genuinely pocket sized, little larger than a microscope slide itself. We have previously proposed the concept of exploiting the small diameter and low cost of these systems to assemble "arrays" of imagers capable of imaging multiple fields of view in parallel to reduce the workload on the microscopist who typically has to survey up to 100 fields before reporting a diagnosis.

The objective lenses presented in this paper could also be integrated into complete POC diagnostic imaging systems which take advantage of low-cost CMOS image sensors and

processing hardware to reduce the workload on overburdened microscopy centers. Use of cell phone hardware offers a very appealing route to portable digital microscopy, and several approaches have been reported for increasing the original camera's resolution to the level required for POC pathology or cytology examination<sup>38</sup>. Systems that add only a single additional lens, such as a ball lens, on top of the phone camera are less expensive, simpler, and smaller than those involving more complex objective lenses, but often have lower resolutions due to their limited ability to correct for aberrations. Some aberrations can be minimized by digitally combining multiple images acquired at different focal planes<sup>1,31</sup>, but this approach is sub-optimal and as we show here can be addressed by careful optical design strategies. Our hybrid objective lenses could be combined with cell phone hardware for microscopy when high resolution (high NA) is desired, and while the lenses presented here are larger than the previously reported ball lenses, at 4 mm diameter they still remain significantly more compact and cost-efficient than a conventional objective lens. While lens-free holography has demonstrated great potential for use in mobile POC diagnostic applications, particularly high-throughput analysis of cells, the approach can encounter difficulties when imaging non-sparse or thick samples, such as a tissue slice or thick blood smear<sup>13</sup>. Use of a compact objective lens to provide high-resolution conventional imaging may be preferred in these applications where lens-free techniques have limitations. We also note that the cost benefits of the hybrid objective design used here derive substantially from the use of optomechanical mountings which inherently provide high precision alignment, thereby reducing assembly costs. These components can be used in lens systems designed to operate with different specifications such as lower NA and larger field of view, depending on the requirements of the target application.

In summary, we have demonstrated that compact microscope objective lenses based on a novel hybrid glass – plastic lens design can be used for imaging biological samples for diagnosis of selected diseases of relevance in point of care diagnostic applications. These optical systems can potentially be mass-produced for under \$10 each and have flexibility to allow integration into a wide range of existing and emerging optical POC diagnostic instrumentation.



## **Acknowledgements**

We thank Dr. Nadarajah Vigneswaran at The University of Texas Health Science Center, Dental Branch, Houston, for his help and expertise in reviewing the oral pathology slides. We also thank Dr. Robert Kester at Rice University for his initial editing input of the paper material. This research was supported by the National Cancer Institute (NCI) under grants R01 CA124319 and R01 CA103830.

## References:

1. Arpa, A., G. Wetzstein, D. Lanman, and R. Raskar. Single lens off-chip cellphone microscopy. IEEE International Workshop on Projector-Camera Systems (PROCAMS) 2012.
2. Barretto, R. P. J., B. Messerschmidt, and M. J. Schnitzer. *In vivo* fluorescence imaging with high resolution microlenses. Nat. Meth. 6:511-512, 2009.
3. Behr, M. A., E. Kokoskin, T. W. Gyorkos, L. Cédilotte, G. M. Faubert, and J. D. MacLean. Laboratory diagnosis for *Giardia lamblia* infection: A comparison of microscopy, coprodiagnosis and serology. Can. J. Infect. Dis. 8:33-38, 1996.
4. Bray, F., B. Møller. Predicting the future burden of cancer. Nat. Rev. Cancer 6:63-74, 2006.
5. Breslauer, D. N., R. N. Maamari, N. A. Switz, W. A. Lam, and D. A. Fletcher. Mobile phone based clinical microscopy for global health applications. PLoS ONE 4:e6320, 2009.
6. Brun, R., J. Blum, F. Chappuis, C. Burri. Human African trypanosomiasis. Lancet 375:148-159, 2010.

7. Camou, S., H. Fujita, and T. Fujii. PDMS 2D optical lens integrated with microfluidic channels: principle and characterization. *Lab Chip* 3:40-45, 2003.
8. Chalmers, R. M., F. Katzer. Looking for *Cryptosporidium*: the application of advances in detection and diagnosis. *Trends Parasitol.* 29:237-251, 2013.
9. Chidley, M. D., K. D. Carlson, R. R. Richards-Kortum, and M. R. Descour. Design, assembly, and optical bench testing of a high-numerical-aperture miniature injection-molded objective for fiber-optic confocal reflectance microscopy. *Appl. Opt.* 45:2545-2554, 2006.
10. Chin, C. D., V. Linder, and S. K. Sia. Lab-on-a-chip devices for global health: Past studies and future opportunities. *Lab Chip* 7:41-57, 2007.
11. Chinowsky, T. M., M. S. Grow, K. S. Johnston, K. Nelson, T. Edwards, E. Fu, and P. Yager. Compact, high performance surface plasmon resonance imaging system. *Biosens. Bioelectron.* 22:2208-2215, 2007.
12. Farmer, P., J. Frenk, F. M. Knaul, L. N. Shulman, G. Alleyne, L. Armstrong, R. Atun, D. Blayney, L. Chen, R. Feachem, M. Gospodarowicz, J. Gralow, S. Gupta, A. Langer, J. Lob-Levyt, C. Neal, A. Mbewu, D. Mired, P. Piot, K. S. Reddy, J. D. Sachs, M. Sarhan, and J. R. Seffrin. Expansion of cancer care and control in countries of low and middle income: a call to action. *Lancet* 376:1186-1193, 2010.

13. Greenbaum, A., W. Luo, T-W. Su, Z. Göröcs, L. Xue, S. O. Isikman, A. F. Coskun, O. Mudanyali, and A. Ozcan. Imaging without lenses: achievements and remaining challenges of wide-field on-chip microscopy. *Nat. Meth.* 9:889-895, 2012.
14. Greenbaum, A., W. Luo, B. Khademhosseini, T-W. Su, A. F. Coskun, and A. Ozcan. Increased space-bandwidth product in pixel super-resolved lensfree on-chip microscopy. *Scientific Reports* 3:1717, 2013.
15. Greenbaum, A., A. Feizi, N. Akbari, and A. Ozcan. Wide-field computational color imaging using pixel super-resolved on-chip microscopy. *Opt. Express* 10:12469-12483, 2013.
16. Industrial Machine Sales, Inc. *personal communication*
17. International Agency for Research on Cancer. *World Cancer Report*. Boyle, P., B. Levin, Eds. Lyon, France. IARC. 2008.
18. Kester, R. T., T. Tkaczyk, M. R. Descour, T. Christenson, and R. Richards-Kortum. High numerical aperture microendoscope objective for a fiber confocal reflectance microscope. *Opt. Express* 15:2409-2420, 2007.

19. Kester, R. T., T. Christenson, R. Richards-Kortum, and T. S. Tkaczyk. Low cost, high performance, self-aligning miniature optical systems. *Appl. Opt.* 48:3375-3384, 2009.
20. Lee, M., O. Yaglidere, and A. Ozcan. Field-portable reflection and transmission microscopy based on lensless holography. *Biomed. Opt. Express* 2:2721-2730, 2011.
21. Lee-Lewandrowski, E., J. L. Januzzi, S. M. Green, B. Tannous, A. H. Wu, A. Smith, A. Wong, M. M. Murakami, J. Kaczmarek, F. S. Apple, W. L. Miller, K. Hartman, and A. S. Jaffe. Multi-center validation of the Response Biomedical Corporation RAMP® NT-proBNP assay with comparison to the Roche Diagnostics GmbH Elecsys® proBNP assay. *Clinica. Chimica. Acta.* 386:20-24, 2007.
22. Liang, C., K. B. Sung, R. R. Richards-Kortum, and M. R. Descour. Design of a high-numerical-aperture miniature microscope objective for an endoscopic fiber confocal reflectance microscope. *Appl. Opt.* 41:4603-4610, 2002.
23. McLeod, E., W. Luo, O. Mudanyali, A. Greenbaum, and A. Ozcan. Toward giga-pixel nanoscopy on a chip: A computational wide-field look at the nano-scale without the use of lenses. *Lab Chip* 13:2028-2035, 2013.
24. Miller, A. R., G. L. Davis, Z. M. Oden, M. R. Razavi, A. Fateh, M. Ghazanfari, F. Abdolrahimi, S. Poorazar, F. Sakhaie, R. J. Olsen, A. R. Bahrmand, M. C. Pierce, E. A.

- Graviss, and R. Richards-Kortum. Portable, battery-operated, low-cost, bright field and fluorescence microscope. *PLoS ONE* 5:e11890, 2010.
25. Minion, J., H. Sohn, and M. Pai. Light-emitting diode technologies for TB diagnosis: what is on the market? *Expert Rev. Med. Devices* 6:341-345, 2009.
26. Myers, F. B., L. P. Lee. Innovations in optical microfluidic technologies for point-of-care diagnostics. *Lab Chip* 8:2015-2031, 2008.
27. Rodriguez, W. R., N. Christodoulides, P. N. Floriano, S. Graham, S. Mohanty, M. Dixon, M. Hsiang, T. Peter, S. Zavahir, I. Thior, D. Romanovicz, B. Bernard, A. P. Goodey, B. D. Walker, and J. T. McDevitt. A microchip CD4 counting method for HIV monitoring in resource-poor settings. *PLoS Med.* 2:663-672, 2005.
28. Seo, J., L. P. Lee. Disposable integrated microfluidics with self-aligned planar microlenses. *Sens. Act. B: Chem.* 99:615-622, 2004.
29. Shirley, D. A., S. N. Moonah, and K. L. Kotloff. Burden of disease from cryptosporidiosis. *Curr. Opin. Infect. Dis.* 25:555-563, 2012.
30. Sia, S. K., V. Linder, B. A. Parviz, A. Siegel, and G. M. Whitesides. An integrated approach to a portable and low-cost immunoassay for resource-poor settings. *Angew. Chem. Int. Ed.* 43:498-502, 2004.

31. Smith Z. J., K. Chu, A. R. Espenson, M. Rahimzadeh, A. Gryshuk, M. Molinaro, D. M. Dwyre, S. Lane, D. Mathews, and S. Wachsmann-Hogiu. Cell-phone-based platform for biomedical device development and education applications. *PLoS ONE* 6:e17150, 2011.
32. Weigum, S. E., P. N. Floriano, S. W. Redding, C. K. Yeh, S. D. Westbrook, H. S. McGuff, A. Lin, F. R. Miller, F. Villarreal, S. D. Rowan, N. Vigneswaran, M. D. Williams, and J. T. McDevitt. Nano-bio-chip sensor platform for examination of oral exfoliative cytology. *Cancer Prev. Res.* 3:518-528, 2010.
33. World Health Organization. *Laboratory Services in TB Control, Microscopy Part II.* Geneva, WHO, 1998.
34. World Health Organization. *Basic Malaria Microscopy: Part I. Learner's guide. Second Edition.* Geneva, WHO, 2010.
35. Wu, A. H., A. Smith, R. H. Christenson, M. M. Murakami, and F. S. Apple. Evaluation of a point-of-care assay for cardiac markers for patients suspected of acute myocardial infarction. *Clinica. Chimica. Acta.* 346:211-219, 2004.
36. Yacoub-George, E., W. Hell, L. Meixner, F. Wenninger, K. Bock, P. Lindner, H. Wolf, T. Kloth, and K. A. Feller. Automated 10-channel capillary chip immunodetector for biological agents detection. *Biosens Bioelectron.* 2007, 22, 1368-1375.

37. Ymeti, A., J. Greve, P. V. Lambeck, T. Wink, S. W. van Hovell, T. A. Beumer, R. R. Wijn, R. G. Heideman, V. Subramaniam and J. S. Kanger. Fast, ultrasensitive virus detection using a Young interferometer sensor. *Nano Lett.* 7:394-397, 2007.
38. Zhu, H., S. O. Isikman, O. Mudanyali, A. Greenbaum, and A. Ozcan. Optical imaging techniques for point-of-care diagnostics. *Lab Chip* 13:51-67, 2012.
39. Zhu, H., O. Yaglidere, T. Su, D. Tseng, and A. Ozcan. Cost-effective and compact wide-field fluorescent imaging on a cell-phone. *Lab Chip* 11:315-322, 2010.



**Table 1:** Technical specifications for the objectives used in this study. \* In volumes of 10,000.

Type	Mag.	NA	WD [mm]	OD [mm]	FoV [mm]	Price	Resolution [ $\mu\text{m}$ ]	DoF [ $\mu\text{m}$ ]
Zeiss, Plan Apo	10x	0.45	2.00	30	2.5	\$2,568	0.75	2.72
Zeiss, Plan Apo	20x	0.75	0.55	33	1.25	\$3,262	0.45	0.98
Zeiss, Plan Apo	40x	0.95	0.25	38	0.625	\$6,789	0.35	0.61
Liang <i>et al.</i> , <sup>22</sup> Fig. 1a	3.33x	1.0	0.45	7	0.25	\$8,000	0.34	0.55
Chidley <i>et al.</i> , <sup>9</sup> Fig. 1b	3.33x	1.0	0.45	7	0.25	\$250*	0.34	0.55
Kester <i>et al.</i> , <sup>19</sup> Fig. 1c	2.86x	1.0	0.45	4	0.25	\$100*	0.34	0.55

**Table 2:** Examples of target diseases for POC tests and microscopic parameters recommended for diagnosis. Numbers of fields to examine refers to the minimum to reach a negative diagnosis.

<b>Disease</b>	<b>Specimen</b>	<b>Diagnostic target</b>	<b>Recommended microscopy</b>	<b>Reference</b>
Malaria	Blood	Parasite 1.5-2.5 $\mu\text{m}$ (ring stage)	100 fields at 100x (thick smear) 800 fields at 100x (thin smear)	34
Trypanosomiasis	Blood	Elongated trypanosome 15-30 $\mu\text{m}$ x 1-3 $\mu\text{m}$	100 fields at 100x (thick smear) 800 fields at 100x (thin smear)	6
Tuberculosis	Sputum	Rod shaped bacilli 1-10 $\mu\text{m}$ long	100 fields at 100x (bright field) 40 fields at 40x (fluorescence)	33
Cryptosporidium	Stool	Round oocysts 4-6 $\mu\text{m}$ diameter	100 fields at 100x (bright field) 40 fields at 40x (fluorescence)	8
Giardia	Stool	Oval cysts 11-14 $\mu\text{m}$ major axis	100x, 150 fields	3

**Table 3:** Cost breakdown of hybrid objective components and assembly.

<b>Cost per objective at various quantities</b>			
<b>Quantity:</b>	<b>10,000</b>	<b>100,000</b>	<b>1,000,000</b>
Glass lens	\$6.00	\$3.00	\$2.00
Plastic lenses	\$6.00	\$1.50	\$0.13
Coatings	\$1.60	\$1.00	\$0.50
Optomechanics	\$81.80	\$3.30	\$3.20
Spacer	\$1.00	\$0.30	\$0.25
Housing	\$1.00	\$0.30	\$0.25
Assembly	\$5.00	\$3.00	\$2.50
<b>Estimated Total:</b>	<b>\$102.40</b>	<b>\$12.40</b>	<b>\$8.83</b>

**Table 4:** Cost comparison of metal opto-mechanics for miniature objectives for prototyping quantities and production quantities.

		<b>Prototyping (4" wafer) X-ray</b>	<b>Prototyping (6" wafer) X-ray</b>	<b>Production (6" wafer) X-Ray</b>	<b>Production (6" wafer) UV</b>	<b>Production (6" wafer) UV</b>
Quantity:		300	1200	1-3 million	1-3 million	10-100 million
Diameter:	Thickness:					
3 mm	500 $\mu\text{m}$	\$30	\$10	\$2.20	\$0.45	\$0.25
	250 $\mu\text{m}$	\$30	\$10	\$1.46	\$0.35	\$0.20
	125 $\mu\text{m}$	\$30	\$10	\$1.15	\$0.30	\$0.15
Quantity:		2400	9600	1-3 million	1-3 million	10-100 million
Diameter:	Thickness:					
1 mm	500 $\mu\text{m}$	\$3.75	\$1.25	\$0.29	\$0.09	\$0.05
	250 $\mu\text{m}$	\$3.75	\$1.25	\$0.19	\$0.07	\$0.04
	125 $\mu\text{m}$	\$3.75	\$1.25	\$0.15	\$0.06	\$0.03

## Figure Legends:

Figure 1: (a) Compact microscope objectives composed of (I) glass lenses, (II) injection-molded plastic lenses, and (III) a hybrid combination of glass and plastic lenses. A standard microscope objective with similar NA and field of view is shown for comparison of scale. (b) Schematic diagram of the experimental configuration used for acquiring images with the hybrid lens.

Figure 2: Images of H&E-stained buccal mucosa tissue section taken with (a) the hybrid objective, and (b) a Zeiss 40x / 0.95 plan-apochromat objective. (c) Comparison of nuclear-to-cytoplasm ratio quantified as a function of depth beneath the epithelial surface in the images shown in (a) and (b).

Figure 3: Images of a malaria-infected human blood smear sample following Giemsa staining, acquired with (a) the hybrid objective, and (b) a Zeiss 40x / 0.95 plan-apochromat objective. (c) Comparison of parasite count determined in three paired fields-of-view, using images acquired by the hybrid and conventional objective systems.

Figure 4: Images of *C. parvum* immunofluorescent-stained oocysts taken with (a) the hybrid miniature objective and (b) a Zeiss 40x / 0.95 plan-apochromat objective. Scale bar = 20  $\mu\text{m}$ . Cross-sectional intensity profiles through individual oocysts from images acquired with (c) the hybrid and (d) conventional objective lenses.

Figure 5: Fabrication costs for the hybrid glass / plastic objective in (a) prototyping and (b) production quantities. The cost of individual lenses assumes use of diamond turning or injection molding techniques for prototyping and production processes, respectively.

Figure 1:

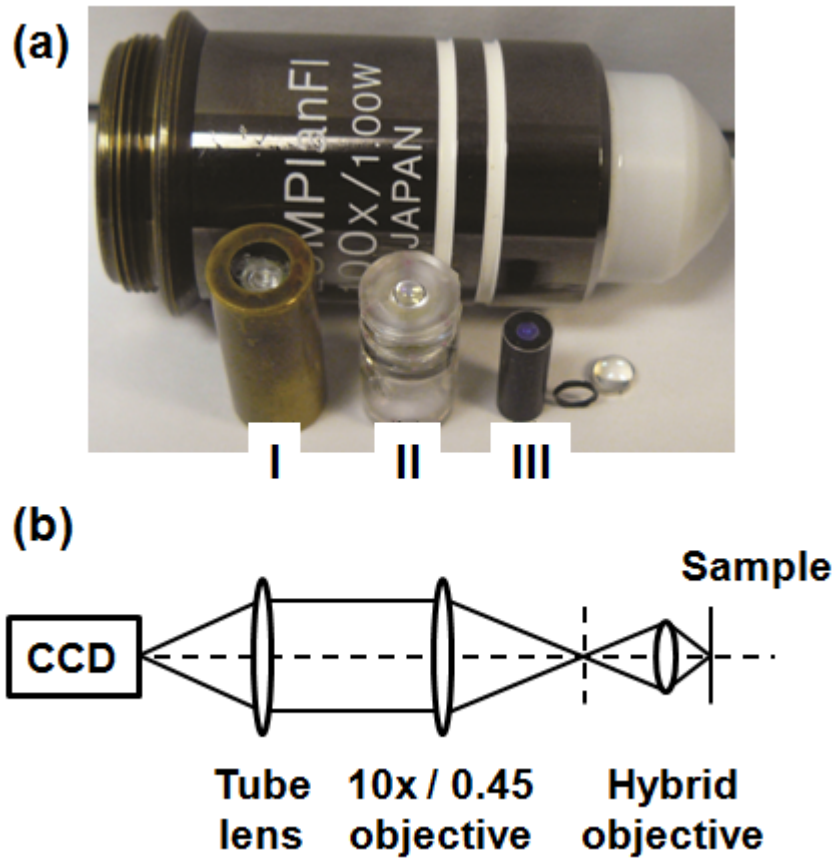


Figure 2:

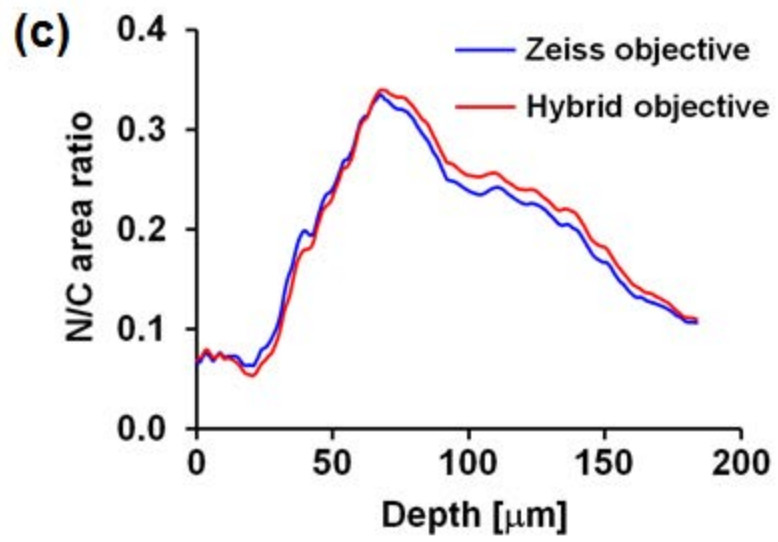
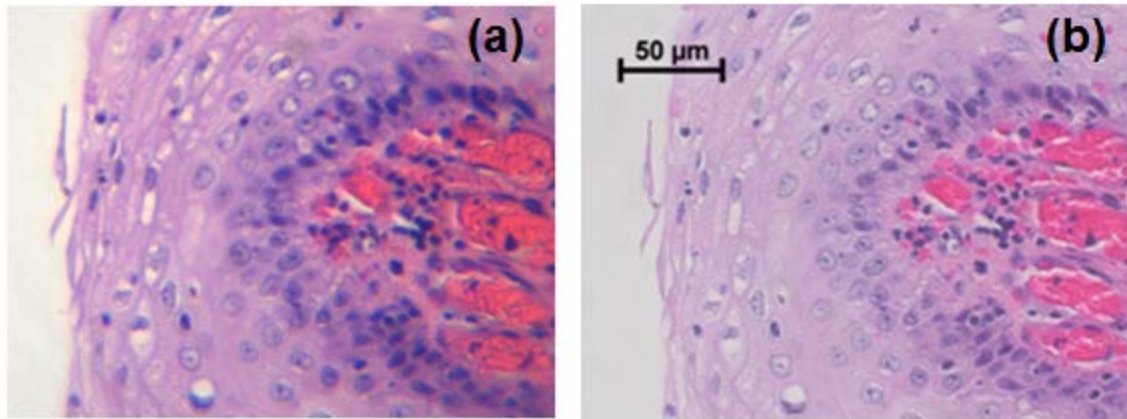




Figure 3:

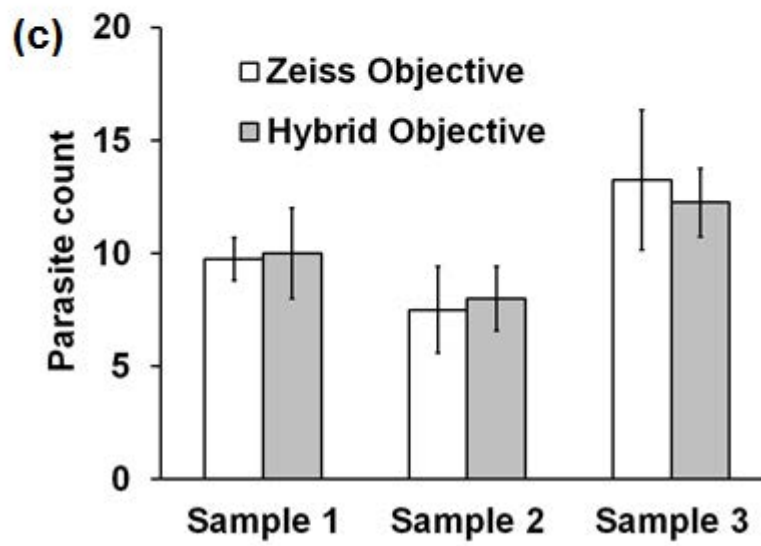
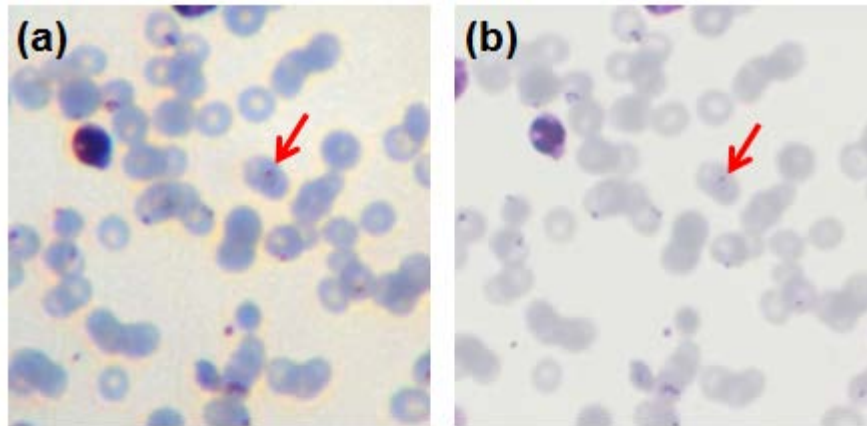


Figure 4:

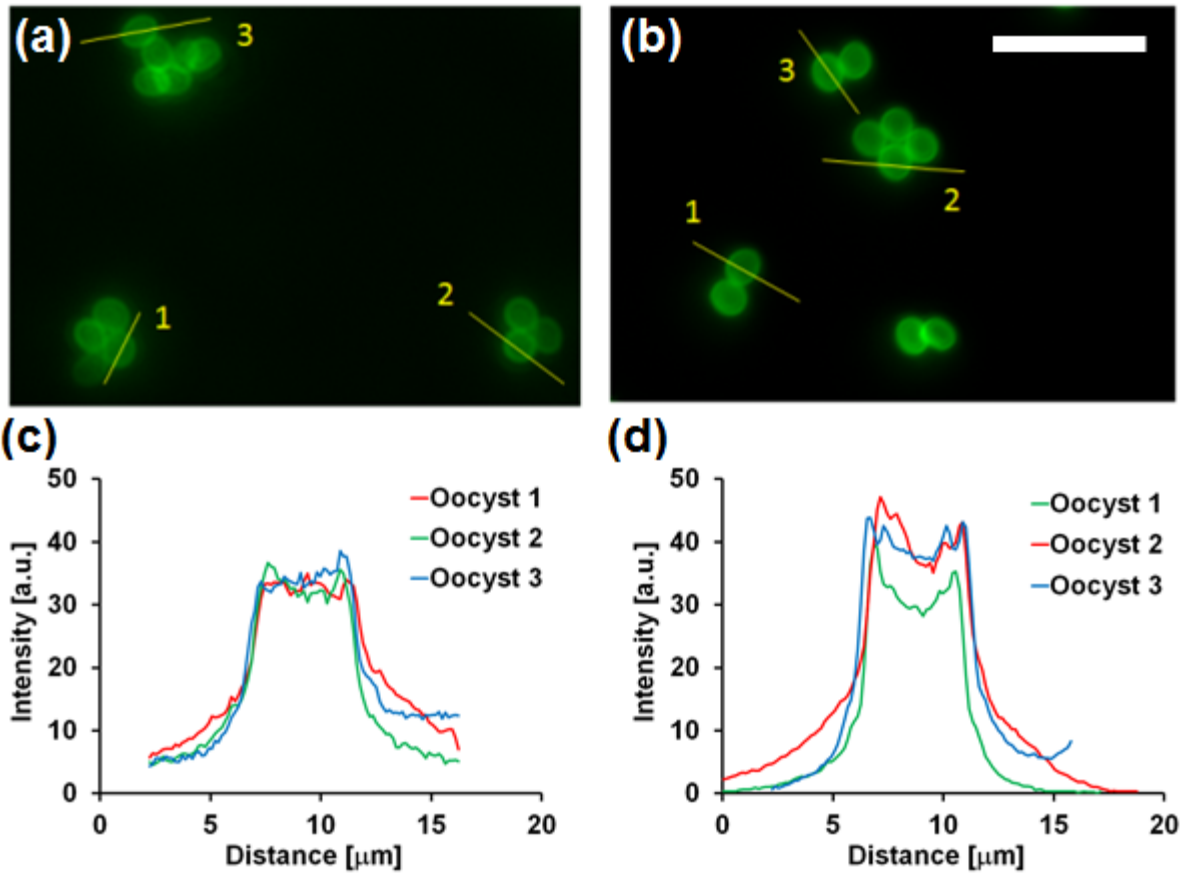


Figure 5:

